

# Measurement of Physical Properties of Anodized Al<sub>2</sub>O<sub>3</sub> FESEM Images

Parashuram Bannigidad  
Dept. of Computer Science,  
Rani Channamma University,  
Belgaum Karnataka India

Jalaja Udoshi  
Dept. of Computer Science,  
Rani Channamma University,  
Belgaum Karnataka India

C. C. Vidyasagar  
Dept. of Chemistry,  
Rani Channamma University,  
Belgaum Karnataka India

## ABSTRACT

The objective of the proposed study is to develop an automated tool to determine the effect of time on nanopore structures. The designed tool extracts the nanopores from the Al<sub>2</sub>O<sub>3</sub> FESEM images and computes their geometrical and statistical features. These values are further used to measure the variance of wall thickness and nanopore size which depend on four prominent anodizing parameters, namely, concentration (%), time (min), temperature (°C) and voltage (V). It is found that the structure and regularity of the nanopore arrangement is significantly improved by increasing anodizing time (min) at constant concentration (%), temperature (°C) and voltage (V). It is also observed that, after the anodizing process at every interval of time there is a significant decrease in wall thickness from 58nm to 41nm and increase in nanopore size from 32nm to 78 nm. The experimental results are compared with the manual results obtained by the chemical expert and demonstrate the efficacy of the proposed method.

## General Terms

Algorithms, Al<sub>2</sub>O<sub>3</sub>, Nanotechnology.

## Keywords

Aluminium nanopore, Computational chemistry, Nanopore image analysis, Image segmentation, FESEM, nanomaterial.

## 1. INTRODUCTION

The nanopore structures have been extensively investigated as the building blocks for various technological applications such as electronics, optoelectronics [1, 2] and sensors [3]. Recently, as an emerging field, NWs have been utilized for energy harvesting devices, for instance, to convert thermal [4], mechanical [5], and solar energy into electricity [6]. On the other hand, the NPL axial and radial junctions provide a three dimensional (3-D) geometric configuration for reduced surface optical reflection and enhanced absorption. The enhanced carrier collection and optical absorption can in principle enable more efficient PVs as compared to planar structures. However, the surface and the interface area enhancement also result in an increase in surface/interface recombination events. The ordering of the NPL arrays may be used as light trapping schemes analogous to random surface texturization or periodic grating couplers in thin films [7]. A porous anodization of aluminium oxide (AAO) template is fabricated for subsequent NPL growth at the bottom of each pore. The AAO template is etched back, exposing the pillars, and the semiconductor absorber layer is then deposited. This process enables the fabrication of an NPL cell on a low-cost Al metal foil. When anodized in an acidic environment with proper process conditions, aluminium oxidizes to form a porous alumina layer consisting of hexagonally packed arrays of nanopores [8], the pores are normal to the aluminium surface and extend from the surface to the

alumina/aluminium interface where there is an oxide barrier layer with near hemispherical geometry. The shape and size of the pores are relatively uniform, with the pitch and diameter being directly proportional to the anodization voltage, and the height controlled by the anodization time. Anodized aluminium oxide (AAO) has proven to be a highly versatile materials system that has found important applications in photonics, energy devices including super capacitors, filtration and purification and architectural and anticorrosive finishes [9-11]. Furthermore, given the uniformity of size-controlled nanopores, AAO has been widely utilized as a template for ordered synthesis of nanostructured materials, including metallic and semiconductor nanorods [12-13], nanowires [14-16], nanotubes [17] and nanoparticles [18]. Importantly, aluminium anodization, in principle, is a highly scalable process as long as a stable voltage and current density are applied with a constant electrolyte temperature, anodization time and composition. The protection or decoration of Al surfaces by anodization has been used commercially since 1923. It is essential to obtain particles or pores with uniform diameters and shapes and, for the purpose of particular applications, to arrange and embed them in a superstructure.

The various applications of nano structures or pores are; size quantization effects, high number of surface atoms, and special surface states, special optical, electronic, magnetic and chemical properties. Some of the biomedical applications are decontamination and antibacterial agents, slow release drugs, filter in hemodialysis, enzyme mimetics and biosensors and adjuvant in anticancer therapy. Self-organized "nanopore" structures in anodic alumina films, called "alumite", have attracted great attention due to their high pore density and their potential use for masking or information storage. When the pores are filled with metals or semiconductors in a subsequent alternating-current reductive electrolysis, these films can be fabricated into interesting magnetic recording, electronic, and electro optical devices [17-19]. By considering these constraints, here demonstrated continuous change in pore diameter, wall thickness and interpore distance as anodization time increases.

Many authors have done their research work in this area; the microscopic image analysis of nanoparticles by edge detection using ant colony optimization has been investigated by Shwetabh Singh [17]. Effect of time on anodized Al<sub>2</sub>O<sub>3</sub> nanopore FESEM images using digital image processing techniques was carried out by Parashuram Bannigidad et al. [20]. Size measurement of nanoparticle assembly using multilevel segmented TEM images (FePt) was investigated by

Paisarn Muneesawang et al. [21]. Detecting subsurface circular objects from low contrast noisy images and its applications in microscope image enhancement was carried out by Soham De et al. [22]. A K-means based methodology for evaluation of

shape parameters for nano-particles was proposed by Ashish Kumar et. al. [23]. Influence of anodizing time on porosity of nanopore structures grown on flexible TLC aluminium films and analysis of images using MATLAB software has been investigated by Vidyasagar et. al. [24]. In this paper, the anodic oxide formed on pure aluminium TLC film without any pre-anneal is investigated and the effects of anodizing time, voltage, concentration and temperature on the structural properties of the oxide films are examined in detail through digital image analysis. The FESEM images of  $Al_2O_3$  films captured at regular intervals of time (A–5 mins, B–9 mins, C–20 mins and D – 30 mins) and constant in concentration, temperature and voltage are shown in the Fig. 1.

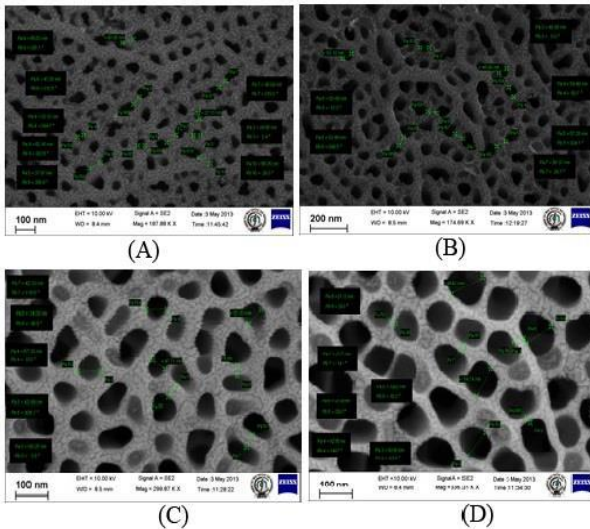


**Fig. 1** FE-SEM images of  $Al_2O_3$  films captured at regular intervals of time (A–5 mins, B–9 mins, C–20 mins and D–30 mins) and constant in concentration, temperature and voltage

Automated microscopic image analysis provides an efficient tool for qualitative analysis in modern material science and biological studies. The main advantages of using digital image processing and pattern recognition techniques in conjunction with microscopy for quantitative studies of anodizing alumina; automatic image analysis reduces the amount of tedious work with microscopes needed to perform a more accurate quantitative analysis and these techniques provide an important quantitative tool to analyze the structures and spatial features of  $Al_2O_3$  films.

## 2. MATERIALS AND METHODS

TLC Silica Gel 60 F254 plates were procured from Merck. Orthophosphoric acid was procured from s-d fine Chem. Ltd. Mumbai. Double distilled water was used throughout the experiments. DC power supply source measure unit was used as the power supply to measure voltage or current simultaneously (Aplab: L6405). MATLAB version 7.9.0.529 (R2009) software, which was installed on PC (hp: G42, 2012) used for image analysis. TLC plates were cut into proper size of 2x4 cm (0.5 mm thickness) of the following chemical composition (wt%): Al 99.79% (Aluminium), Cu 0.05% (Copper), Mg 0.05% (Magnesium), Si 0.05% (Silicon), Mn 0.05% (Manganese) and Zn 0.01% (Zinc). Coated silica was removed by rubbing the surface using emery sheet grit 600. The Al plates were washed with distilled water, rinsed with ethanol, degreased with acetone in ultrasonic bath for 15 min. Finally, the Al plates were purged by distilled water in ultrasonic bath for another 10 min. Before anodizing, the

electrochemical polishing of samples was carried out in a 0.75M NaOH solution. Al plates were immersed in NaOH solution for 4 min to remove alkaline impurities. The samples were rinsed with distilled water and acetone. Later Al plates were rinsed thoroughly and kept undisturbed in distilled water for 10 min. Anodization was performed in a conventional cell using a platinum helical wire as a cathode. Al was used as the counter-electrode, and typically about 90% of the Al was immersed in the electrolyte while the exposed one was connected to the anode through a crocodile clips. The electrical contact was made at the edge of the electrodes. Pt electrode served as the cathode electrode and the distance from the anode electrode was 3 cm. The samples were anodized in an acidic aqueous solution at different time interval at constant concentration and voltage. Ice cold water was used to maintain low temperatures using thermometer. During anodization the electrolyte was kept undisturbed, and the values of voltage, current, time and temperature were recorded. After the anodization process, the samples were rinsed thrice in deionized water and acetone and dried at 90 °C for 1 hour in an oven and was wrapped in aluminium foil. The variation in the time could be attributed to change in the pore size and wall thickness of the anodized  $Al_2O_3$  thin films.

## 3. PROPOSED METHOD

The objective of the present study is to develop an automatic tool to determine the effect of time on nanopore structures formed via electrochemical anodization of high purity  $Al_2O_3$  films in digital microscopic (Field Emission Scanning Electron Microscope (FESEM) nanopore images. The geometrical and statistical shape features tend to vary with the different anodization parameters, namely, concentration (%), time (min), temperature (°C) and voltage (V). In this paper, an automated method is proposed to depict the effect of time on nanopore structures formed via electrochemical anodization of high purity  $Al_2O_3$  films in digital microscopic nanopore images.

The geometric shape features; length, width, area and nanopore diameter of  $Al_2O_3$  nanopore images are defined as below:

**Length:** The longer side of smallest circumscribed rectangle.

**Width:** The shorter side of smallest circumscribed rectangle.

**Area:** The number of pixels belonging to the object provides a measure of the object size.

**Nanopore diameter ( $D_p$ ):** The average ratio of major axis and minor axis.

**Interpore Distance ( $D_i$ ):** The average ratio of neighboring nanopore centroid distance.

The flow diagram of the proposed method is depicted in the below Fig 2:

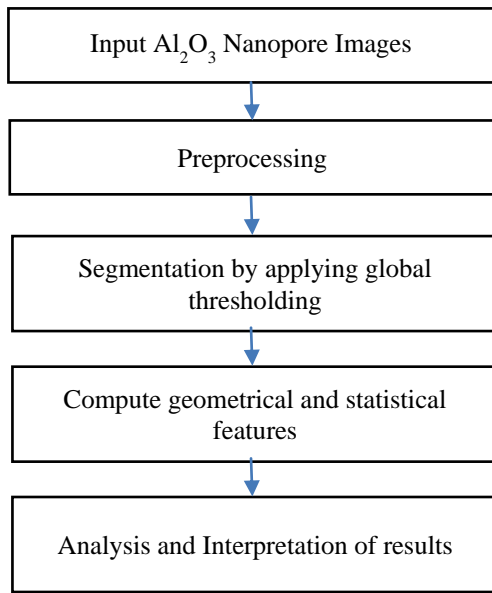


**Fig. 2 Flow diagram of proposed method**

The algorithm for segmentation and feature extraction of nanopore regions of FESEM images is given below:

**Algorithm:** Segmentation and feature extraction of nanopore regions:

*Step 1: Input nanopore FESEM image.*

*Step 2: Perform pre-processing operations on input image (image enhancement and morphological operations).*

*Step 3: Perform segmentation by applying global thresholding on pre-processed image to obtain binarized image (0 representing background and 1 representing objects) and label the objects.*

*Step 4: Compute geometric shape features; length, width, area, pore diameter, interpore distance and wall thickness for each labeled object on step 3.*

*Step 5: Repeat the steps 1 - 4 for all objects.*

*Step 7: Analyze and interpret the results.*

## 4. EXPERIMENTAL RESULTS AND DISCUSSION

The experimentation of the proposed method is carried on Intel(R) Core(TM) Duo T6670 @ 220GHz with 2GB RAM using MATLAB R2010b software. Every Al<sub>2</sub>O<sub>3</sub> FESEM image used in the experiment are captured at regular intervals of time (min) keeping concentration (%), temperature (°C) and voltage (V) constant (Fig. 3. (i)). The input images are converted into gray scale image (Fig. 3 (ii)) and morphological operations such as erosion, reconstruction and dilation are applied. Then performed segmentation by applying global thresholding (Fig. 3 (iii)) to separate background and foreground (nanopores). Geometric shape features, i.e., length, width, area, pore diameter and interpore distance was computed for each labelled segment. Finally, the results are interpreted and compared with manual results obtained by the chemical experts and these results are shown in the Table 2. The details of chemical compositions used for preparation of Al<sub>2</sub>O<sub>3</sub> nanopores during synthesis are given in the Table 1.

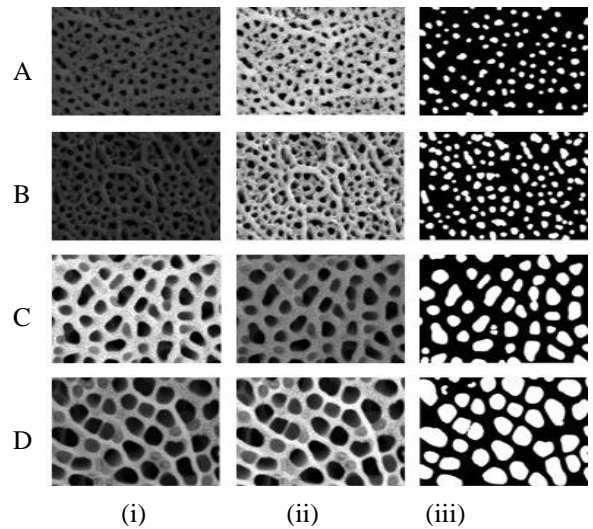


**Fig 3: (i) Original FESEM images at different time intervals, (ii) Gray scale images, (iii) Segmented images**

**Table 1. The details of chemical compositions for preparation of Al<sub>2</sub>O<sub>3</sub> nanopore**

Image	Concentration (%)	Time (min)	Temp (°C)	Velocity (V)
A	5	5	20	50
B	5	9	20	50
C	5	20	20	50
D	5	30	20	50

It is observed that, if the anodization time (min) increases keeping the concentration (%), temperature (°C) and voltage (V) constant, the pore size increases and the wall thickness decreases. The manual results obtained by chemical experts and computed results of time versus wall thickness is depicted in the Fig. 4. Similarly, the results of time versus nanopore size are shown in the Fig. 5. Finally, the effect of anodizing time on wall thickness and pore diameter of the Al<sub>2</sub>O<sub>3</sub> films are shown in the Fig.6.

**Table 2. Geometric feature values of Al<sub>2</sub>O<sub>3</sub> nanopore images of Fig. 4**

Image	Wall Thickness (nm)		Pore Size (nm)	
	Manual	Proposed	Manual	Proposed
A	58	58	32	32.00
B	56	57	34	34.74
C	48	49	58	61.25
D	26	41	81	78.62

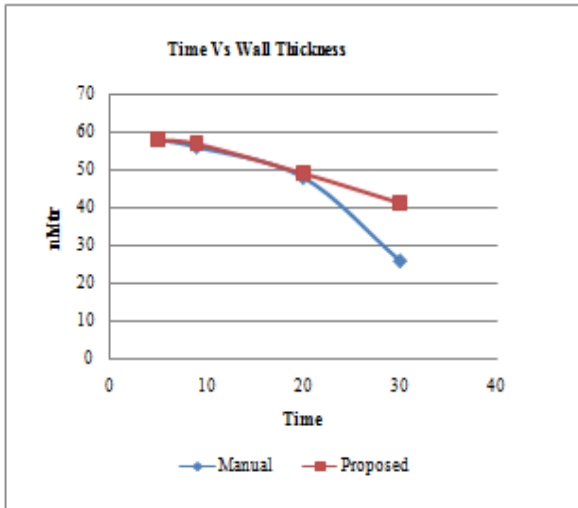


Fig. 4 Time versus nanopore wall thickness of Al<sub>2</sub>O<sub>3</sub> image

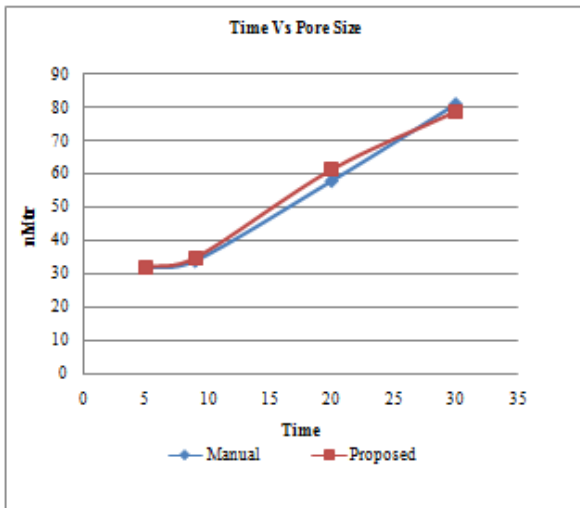


Fig. 5 Time versus nanopore size of Al<sub>2</sub>O<sub>3</sub> image

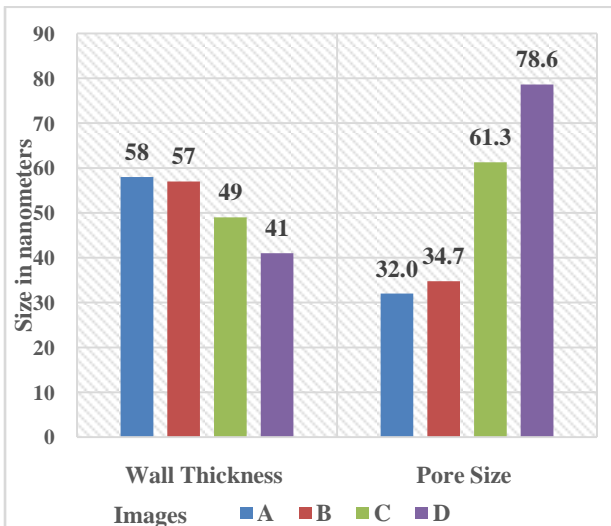


Fig. 6 The effect of anodizing time on wall thickness and nanopore diameter of the Al<sub>2</sub>O<sub>3</sub> films

## 5. CONCLUSION

In this paper, an automated method is proposed to measure the effect of anodization time on nanopore structures formed via electrochemical anodization of high purity Al<sub>2</sub>O<sub>3</sub> films in digital microscopic nanopore images. The geometric shape features like length, width, area, and interpore distance are extracted and computed. It is found that the structure and regularity of nanopores arrangement is significantly improved by increasing anodizing time (min) at constant concentration (%), temperature (°C) and voltage (V). It is also observed that, after the anodizing process at every interval of time there is a significant decrease in wall thickness from 58nm to 41nm and increase in nanopore size from 32nm to 78nm. The experimental results are compared with the manual results obtained by the chemical expert and demonstrate the efficiency of the proposed method. The future scope of the research is to compute porosity and design fuzzy inference rules to predict the wall thickness and pore size for various time intervals at constant concentration, temperature and voltage.

## 6. REFERENCES

- [1] Zhong, Z. H., Qian, F., Wang, D. L., Lieber, C. M. Synthesis of P-Type Gallium Nitride Nanowires for Electronic and Photonic Nanodevices. *Nano Lett.* 2003, 3, 343-346.
- [2] Qian, F., Gradecak, S., Li, Y., Wen, C. Y., Lieber, C. M. (2005). Core/Multishell Nanowire Heterostructures as Multicolor, High-Efficiency Light-Emitting Diodes. *Nano Lett.* 5, 2287-2291.
- [3] Fan, Z. Y., Wang, D. W., Chang, P. C., Tseng, W. Y., Lu, J. G. (2004). ZnO Nanowire Field Effect Transistor And Oxygen Sensing Property. *Appl. Phys. Lett.* 85, 5923-5937.
- [4] Hochbaum, A. I., Chen, R. K., Delgado, R. D., Liang, E. C., Garnett, W. J., Najarian, M., Majumdar, A., Yang, P. D. (2008). Enhanced Thermoelectric Performance Of Rough Silicon Nanowires. *Nature*, 451, 163-167.
- [5] Wang, Z. L., Song, J. H. (2006). Piezoelectric Nanogenerators Based On Zinc Oxide Nanowire Arrays. *Science*, 312, 242-246.
- [6] Fan, Z. Y., Razavi, H., Do, J. W., Moriwaki, A., Ergen, O., Chueh, Y. L., Leu, P. W., Ho, J. C., Takahashi, T., Reichertz, L. A., Neale, S., Yu, K., Wu, M., Ager, J. W., Javey, A. (2009). Three-Dimensional Nanopillar-Array Photovoltaics On Low-Cost And Flexible Substrates. *Nature Mater.* 8, 648-653.
- [7] Stiebig, H., Senoussaoui, N., Zahren, C., Haase, C., Muller, J. Prog. (2006). Silicon Thin-Film Solar Cells With Rectangular-Shaped Grating Couplers. *Photovoltaics*, 14, 13-24.
- [8] Masuda, H., Fukuda, K. (1995). Ordered Metal Nanohole Arrays Made by a Two-Step Replication of Honeycomb Structures of Anodic Alumina. *Science*, 268, 1466-1468.
- [9] Banerjee, P., Perez, I., Henn-Lecordier, L., Lee, S. B., Rubloff, G. W. (2009). Nanotubular metal-insulator-metal capacitor arrays for energy storage. *Nat. Nanotechnol.* 4, 292-296.
- [10] Liang, Y., Schwab, M. G., Zhi, L., Mugnaioli, E., Kolb, U., Feng, X., Meullen, K. J. (2010). Direct Access to Metal or Metal Oxide Nanocrystals Integrated with One-

- dimensional Nanoporous Carbons for Electrochemical Energy Storage. *Am. Chem. Soc.* 132, 15030-15037.
- [11] Min Hyung, L., Namsoo, L., Daniel Ruebusch, J., Jamshidi, A., Kapadia, R., Lee, R., Joon Seok, T., Takei, K., Young Cho, K., Fan, Z., Jang, H., Wu, M., Cho, G., Javey, A. (2011). Roll-to-Roll Anodization and Etching of Aluminum Foils for High-Throughput Surface Nanotexturing. *Nano Lett.* 11, 3425-3430.
- [12] Kumar, G., Tang, H. X., Schroers, J. (2009). Nanomoulding with Amorphous Metals *Nature*, 457, 868-872.
- [13] Lyvers, D. P., Moon, J. M., Kildishev, A. V., Shalaev, V. M., Wei, A. (2008). Gold Nanorod Arrays as Plasmonic Cavity Resonators. *ACS Nano*, 2, 2569.
- [14] Vlassiouk, I., Krasnoslobodtsev, A., Smirnov, S., Germann, M. (2008). Direct detection and separation of DNA using nanoporous alumina filters. *Langmuir*, 2004, 20, 9913-9915.
- [15] Diggle, J. W., Downie, T. C., Goulding, C. W. (1969). Anodic oxide films on aluminum *Chem. Rev.* 69, 365-405.
- [16] Feiyue, L., Zhang, R., Metzger, M. (1998). On the Growth of Highly Ordered Pores in Anodized Aluminum Oxide. *Chem. Mater.* 10, 2470-2480.
- [17] Shwetabh, S. (2013). Microscopic Image Analysis of Nanoparticles by Edge Detection Using and Colony Optimization. *J. Computer Eng.* 11, 84-89.
- [18] Fisker, R., Carstensen, J. M., Hanshen, M. F., Bodker, F., Morup, S. (2000). Estimation of nanoparticle size distributions by image analysis. *J. Nanoparticle Res.* 2, 267-277.
- [19] Rafael, C. G., Richard, E. W. (2002). *Digital Image Processing*; Pearson Education Asia
- [20] Parashuram Bannigidad, C. C. Vidyasagar (2015), Effect of Time on Anodized Al<sub>2</sub>O<sub>3</sub> Nanopore FESEM Images using Digital Image Processing Techniques: A Study on Computational Chemistry *IJETTCS*, ISSN 2278-6856, 4, 3, 15-22.
- [21] Paisarn Muneesawang, Chitnarong Sirisathitkul (2015) Size Measurement of Nanoparticle Assembly Using Multilevel Segmented TEM Images, *Journal on Nanomaterials*, Hindawi Publishing Corporation, Article ID 790508, 8.
- [22] Soham De, Nupur Biswas, Abhijit Sanyal, Pulak Ray and Alokmay Datta (2012) Detecting Subsurface Circular Objects from Low Contrast Noisy Images: Applications in Microscope Image Enhancement, *IJCEACIE*, 6, 7.
- [23] Ashish Kumar, Priyadarshni, Preeti Kaushik (2014) A Kmeans Based Methodology for Evaluation of shape parameters for nano-particles, *IJARCSSE*, 4, 1.
- [24] C. C. Vidyasagar, Parashuram Bannigidad, H. B. Muralidhara (2016) Influence of anodizing time on porosity of nanopore structures grown on flexible TiAluminium films and analysis of images using MATLAB software, *Adv. Mater. Lett.* VBRI Press, 7(1), 71-77.